

Phase-dependent field-free molecular alignment and orientationChaochao Qin,^{1,*} Yuzhu Liu,^{2,3,†} Xianzhou Zhang,¹ and Thomas Gerber²¹*Department of Physics, Henan Normal University, 453007 Xinxiang, People's Republic of China*²*Paul Scherrer Institute, 5232 Villigen, Switzerland*³*College of Physics and Optoelectronic Engineering, Nanjing University of Information Science and Technology, 210044 Nanjing, P. R. China*

(Received 19 June 2014; published 24 November 2014)

We investigated the temporal behavior of alignment and orientation of LiH following a femtosecond laser pulse excitation comprising two fields at center frequencies ω and 2ω (e.g., $E(t) = E[\cos(\omega t) + \cos(2\omega t + \Phi)]$) shifted by a phase Φ . The effects of repopulations and rephasing of rotational states on the resulting alignment and orientation were evaluated. The population distribution of rotational states is only changed during the exciting pulse. Afterwards the established rotational state distribution is maintained in the absence of collisions. The phases of rotational states play the most crucial role in determining the time evolution of molecular alignment and orientation. Equal alignment and rotational populations are obtained when the phases are chosen $\Phi = 0$ and $\Phi = \pi$. However, orientation is different due to the fact that in the case $\Phi = \pi$ the mutual phases of even rotation states are not changed but the phases of odd rotational states are shifted by π , comparing with that of $\Phi = 0$. The effect of temperature on molecular orientation was also addressed. It was shown that an efficient field-free molecular orientation can be observed even at room temperature.

DOI: [10.1103/PhysRevA.90.053429](https://doi.org/10.1103/PhysRevA.90.053429)

PACS number(s): 33.80.Rv, 37.10.Vz

I. INTRODUCTION

Laser-induced molecular alignment of small molecules in the gas phase is now routinely applied as femtosecond pump-probe technique [1–3] used for revealing molecular structures [4], controlling and tracing chemical reactions [5–7], generating high-order harmonics [8], and measuring ultrashort laser pulses [9]. However, laser-induced molecular orientation [10] and its periodic revival in the field-free time following a laser pulse excitation is a challenging topic and much less studied experimentally.

Several methods have been proposed to realize molecular orientation, including a strong dc field (e.g., a hexapole field [11] and a strong static electric field [12]), an intense laser field combined with a weak dc field [13], or an asymmetric laser field (that is, the electric field is not symmetric with respect to the time axis, e.g., a THz few-cycle laser field [14–16] or a half-cycle laser field [17–21]), and some arrangements have been experimentally demonstrated [22–26]. Among the above-mentioned techniques, the one using a strong dc field only works if the investigated molecule exhibits a permanent dipole. The one using an intense laser field combined with a weak dc field or an asymmetric laser field are based on the polarizability and hyperpolarizability interaction and works even in the absence of a permanent dipole. In a two-color laser field [27–30] the interaction with a permanent dipole averages out and can be neglected. The observed molecular orientation is then due to the molecular polarizability and hyperpolarizability. The use of two-color fields has been proven to be one of the most versatile methods for molecular orientation and the molecular orientation can be achieved in both nonadiabatic and adiabatic regimes, i.e., with field interaction times shorter or longer than the rotational period, respectively. Especially, the nonadiabatic

molecular orientation can be used to produce the field-free oriented molecules, and so it is desirable for applications in which subsequent interactions with a molecular system are to be investigated. The phase Φ is an important parameter characterizing the electric structure of the femtosecond two-color laser pulse. However, more study is needed on the effect of phase on the population and phase of rotational states in field-free molecular alignment and orientation.

In this paper, we investigate theoretically the phase-dependent effect of initial excitation on the reviving of field-free molecular alignment and orientation following a femtosecond two-color laser pulse in detail, taking a LiH diatomic molecule exhibiting a large molecular permanent dipole and second-order hyperpolarizability as an example. Firstly, we study the dependence of field-free molecular alignment and orientation on the phase of the femtosecond two-color laser pulse. Next, we investigate the populations and phases of rotational states and their effects on molecular alignment and orientation depending on the phase Φ . Finally, we discuss the effect of rotational temperature on molecular alignment and orientation.

II. THEORETICAL METHODS

We consider the control of a linear molecule by use of a nonresonant femtosecond two-color linearly polarized laser pulse given by

$$E(t) = E_0 \exp\left(-2 \ln 2 \frac{t^2}{\tau^2}\right) [\cos \omega t + \cos(2\omega t + \Phi)], \quad (1)$$

where ω is the carrier wave frequency, E_0 is the field amplitude, τ is the pulse duration of the laser pulse, and Φ is the phase, which determines the electric field structure of the laser pulse. When a linear molecule is exposed to the field $E(t)$ defined in Eq. (1), the time-dependent Schrödinger equation can be

*qinch@hotmail.com

†yuzhu.liu@gmail.com

expressed as [31]

$$i\hbar \frac{\partial \psi(t)}{\partial t} = \hat{H}(t)\psi(t), \quad (2)$$

with

$$\begin{aligned} \hat{H}(t) = & B\hat{J}^2 - \mu E(t) \cos \theta - \frac{1}{2}[(\alpha_{\parallel} - \alpha_{\perp})\cos^2 \theta + \alpha_{\perp}]E^2(t) \\ & - \frac{1}{6}[(\beta_{\parallel} - 3\beta_{\perp})\cos^3 \theta + 3\beta_{\perp} \cos \theta]E^3(t), \end{aligned} \quad (3)$$

where B is the rotational constant, \hat{J}^2 denotes the squared angular momentum operator, μ is the permanent dipole moment, θ is the angle between the molecular axis and the laser polarization, α_{\parallel} and α_{\perp} are the polarizability components parallel and perpendicular to the molecular axis, and β_{\parallel} and β_{\perp} are the second-order hyperpolarizability components parallel and perpendicular to the molecular axis.

We expand the rotational wave function using the finite basis set of $|J, M\rangle$, which is a set of the eigenfunctions of a rigid rotor in a field-free space. The polarization axis of the laser pulse is defined as the laboratory-fixed Z axis about which the Hamiltonian is cylindrically symmetric. Accordingly, the magnetic quantum number M is conserved, that is, $\Delta M = 0$, and the wave function is expressed as

$$|\psi(t)\rangle = \sum_{J=0}^{J_{\max}} c_{J,M}(t)|J, M\rangle. \quad (4)$$

J_{\max} is set at the value that far exceeds the highest rotational states excited by the femtosecond laser pulse. In the simulation, the time-dependent Schrödinger equation is numerically solved by the split-operator method [32–35]. Once the wave function $|\psi(t)\rangle$ is known, the expansion coefficients can be calculated from

$$c_{J,M}(t) = \langle J, M | \psi(t) \rangle, \quad (5)$$

where the expansion coefficients $c_{J,M}(t)$ are complex in general and both their moduli and phases, corresponding to the populations and phases of rotational states J , vary during the interaction with the laser.

The corresponding molecular alignment and orientation dynamics are estimated from the obtained wave function as follows:

$$\langle \cos^n \theta \rangle(t) = \langle \psi(t) | \cos^n \theta | \psi(t) \rangle, \quad (6)$$

where $n = 1$ for orientation and $n = 2$ for alignment.

III. RESULTS AND DISCUSSION

In our calculation, the grid number is $N_{\theta} = 50$, time step is $\delta t = 0.01$ fs, and all the calculations converge correctly. The relevant parameters for the femtosecond two-color laser pulse are $\tau = 100$ fs, $\lambda_{\omega} = 800$ nm, $\lambda_{2\omega} = 400$ nm, and $I = 5.0 \times 10^{13}$ W/cm². The molecular parameters of LiH are $\mu = 1.958 \times 10^{-29}$ Cm, $\alpha_{\parallel} = 4.254 \times 10^{-40}$ C² m² J⁻¹, $\alpha_{\perp} = 4.881 \times 10^{-40}$ C² m² J⁻¹, $\beta_{\parallel} = 2.019 \times 10^{-50}$ C³ m³ J⁻², $\beta_{\perp} = 7.502 \times 10^{-51}$ C³ m³ J⁻² [36,37]. The rotational constant of LiH in its vibronic ground state is $B = 7.513$ cm⁻¹. Because the 800 nm and 400 nm are nonresonant to electronic states for LiH, it is hard to excite the molecules to highly excited states like the repulsive states leading to dissociation [38], as shown in Fig. 1.

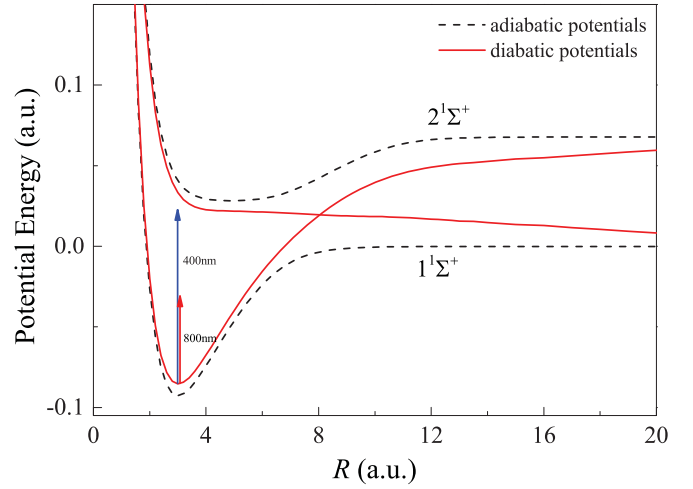


FIG. 1. (Color online) The adiabatic and diabatic potentials for the ground molecular state $1^1\Sigma^+$ and first excited state $2^1\Sigma^+$ of LiH.

Figures 2(a) and 2(b) show the time evolution of the molecular alignment $\langle \cos^2 \theta \rangle$ and molecular orientation $\langle \cos \theta \rangle$ for a cold molecule taking $|J = 0, M = 0\rangle$ as the initial state, assuming phase $\Phi = 0$ in the calculation. The horizontal axis represents time with $t = 0$ at the peak of the femtosecond two-color laser pulse envelope. Molecular alignment and

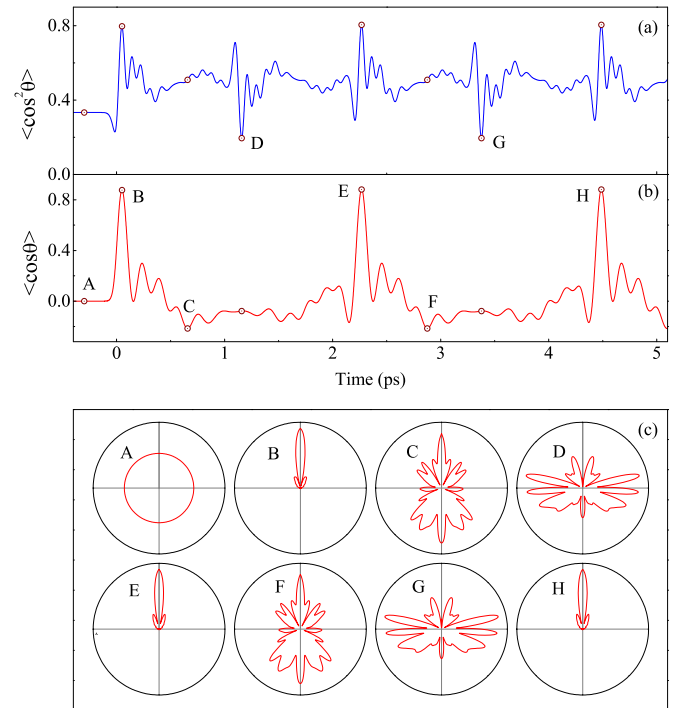


FIG. 2. (Color online) (a) Time evolution of molecular alignment $\langle \cos^2 \theta \rangle$, (b) Time evolution of molecular orientation $\langle \cos \theta \rangle$ and (c) polar plot representation of the angular distribution at different times indicated in (a) and (b) for an ensemble of LiH molecules at the rotational temperature of 0 K by a femtosecond two-color laser pulse with the laser intensity of 5.0×10^{13} W/cm², the pulse duration of 100 fs, and $\Phi = 0$. The linear polarizations of the femtosecond two-color laser pulse are aligned vertically in the plane of the figure.

orientation with impressive values of $\langle \cos^2\theta \rangle_{\max} = 0.805$ and $\langle \cos\theta \rangle_{\max} = 0.881$, respectively, are obtained after the field-molecule interaction and at revival instances with a period of $T_{\text{rot}} = 2.219$ ps. The molecular alignment reaches the maximum at the same time as the positive orientation value. A polar plot of angular distributions of a coherent superposition of rotational states at times denoted A–H in Figs. 2(a) and 2(b) are depicted in Fig. 2(c) and gives further insight into the time evolution of molecular axes. The laser pulse causes rotational excitations; thus the angular momentum of LiH changes in the presence of the electric field, while $\Delta M = 0$. Accordingly, this excitation brings the molecules from a completely isotropic angular distribution to a more aligned and oriented configuration. At A, the molecules are distributed isotropically. At B and E, optimal molecular alignment and orientation are reached together 49fs after the peak intensity of the laser field. At C and F, molecular orientation reaches a minimum with $\langle \cos\theta \rangle = -0.216$ and the molecular alignment $\langle \cos^2\theta \rangle = 0.509$. At D and G, the molecules are antialigned $\langle \cos^2\theta \rangle = 0.196$ and $\langle \cos\theta \rangle = -0.078$. Thus, the angular distributions run through a variety of spatial asymmetries with periodic revival, indicating that the rotational wave packet evolves freely after the laser pulse is over. In the simulations, $\langle \cos\theta \rangle_{\max} > 0$ corresponds to the case when Li atoms are directed in the positive direction of the laboratory-fixed Z axis, (i.e., the positive direction of the electric field). The minimal value, which corresponds to the orientation directed in the negative direction, is estimated to be $\langle \cos\theta \rangle_{\min} = -0.216$. Thus, the orientation dynamics is asymmetric. In addition, we also calculate the single contributions of the permanent dipole moment, the molecular anisotropic polarizability, and the molecular hyperpolarizability interacting with the laser field, respectively. We find that the effects of the hyperpolarizability interaction are the main driving forces in molecular alignment and orientation, and the contribution of the polarizability interaction cannot be neglected. In contrast, for the case of the THz few-cycle field, the main contribution is the permanent dipole moment interaction [15].

The molecular alignment and orientation exhibits a dependence on the phase Φ between the two components of the two-color laser pulse. Figure 3(a) shows the field-free orientation of LiH as a function of the phase Φ at temperature $T = 0$ K. Different phases lead to different degrees of asymmetry between the positive and negative maximum orientation, as shown in Fig. 3(b). It is interesting to note that there exists an exact relation

$$\langle \cos\theta \rangle_{\max} |_{\Phi=\Phi_0} = -\langle \cos\theta \rangle_{\min} |_{\Phi=\pi \pm \Phi_0}. \quad (7)$$

It implies that the direction of orientation can be controlled by changing phase Φ by π , which can be established by fine-tuning the delay time between the two laser field components, as demonstrated in the experiment [39]. Alternatively, the phase shift Φ can be determined by observing the change in the direction of orientation. It should be pointed out that direct measurement of the phase between the 800- and 400-nm laser pulse is a real challenge. The dependence of field-free orientation on the phase Φ opens a way to determine the phase of femtosecond two-color laser pulse.

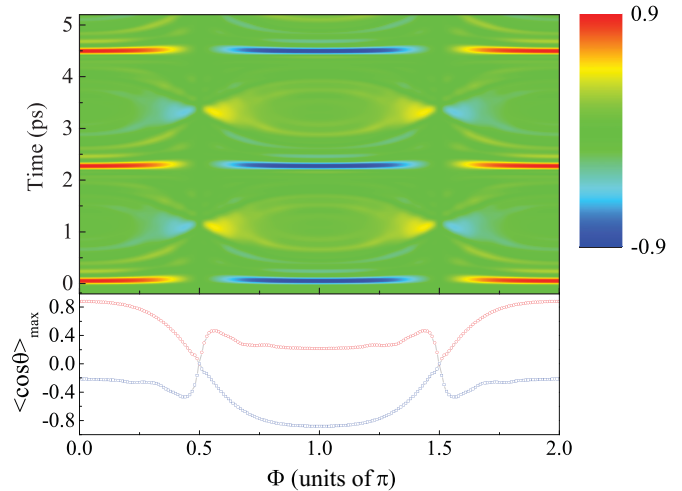


FIG. 3. (Color online) (a) Degree of molecular orientation $\langle \cos\theta \rangle$, (b) maximum degrees of molecular orientation as a function of the phase Φ .

To gain more insights into the effects of Φ on molecular alignment and orientation at the rotational temperature 0 K, we show the field-free molecular alignment and orientation for the case of $\Phi = 0.5\pi$ in Figs. 4(a) and 4(b), respectively. In this case, molecular orientation does not establish and the time

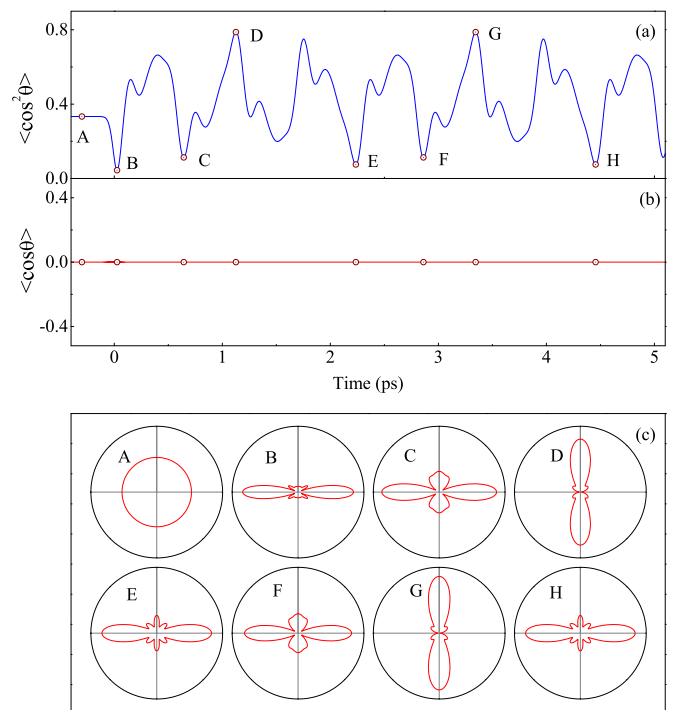


FIG. 4. (Color online) (a) Time evolution of molecular alignment $\langle \cos^2\theta \rangle$, (b) time evolution of molecular orientation $\langle \cos\theta \rangle$, and (c) polar plot representation of the angular distribution at different times indicated in (a) and (b) for an ensemble of LiH molecules at the rotational temperature of 0K by a femtosecond two-color laser pulse, the parameter of which is the same as those used in Fig. 1 except that $\Phi = 0.5\pi$. The linear polarizations of the femtosecond two-color laser pulse are aligned vertically in the plane of the figure.

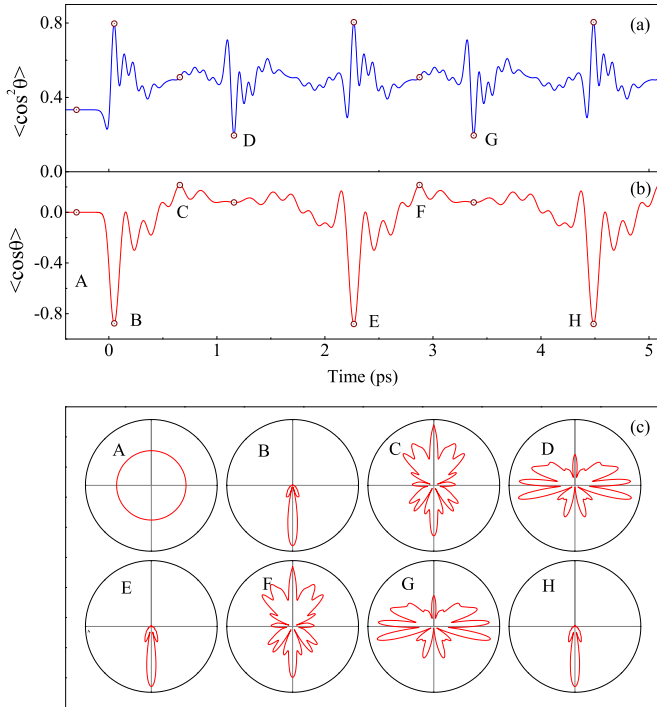


FIG. 5. (Color online) (a) Time evolution of molecular alignment $\langle \cos^2 \theta \rangle$, (b) time evolution of molecular orientation $\langle \cos \theta \rangle$, and (c) polar plot representation of the angular distribution at different times indicated in (a) and (b) for an ensemble of LiH molecules at the rotational temperature of 0 K by a femtosecond two-color laser pulse, the parameter of which is the same as those used in Fig. 1 except that $\Phi = \pi$. The linear polarizations of the femtosecond two-color laser pulse are aligned vertically in the plane of the figure.

evolution of molecular alignment exhibits a less oscillatory time evolution and the duration of alignment for $\langle \cos^2 \theta \rangle > 0.5$ is larger, comparing the results that are shown in Fig. 2. In contrast, it was found that there was no significant dependence of the molecular alignment on the phase between the two colors of the pump pulse for CO molecule [30]. It is probably that LiH has a large molecular permanent dipole and second-order hyperpolarizability, comparing with CO. Moreover, we also show the calculated results for the case of $\Phi = \pi$ in Fig. 5. It is found that the time evolution of molecular alignment is the same as that in Fig. 2(a) but molecular orientation is just the opposite of that in Fig. 2(b).

To demonstrate the physical mechanism of the field-free molecular alignment and orientation induced by the two-color laser pulse and the inherent physical mechanism of the same molecular alignment but opposite molecular orientation for the phase of $\Phi = 0$ and $\Phi = \pi$, we firstly track the population of each rotational state. It is observed that the population of rotational states established during the laser pulse remains unchanged after pulse excitation and the distributions of rotational states for the case of $\Phi = 0$, $\Phi = 0.5\pi$, and $\Phi = \pi$ are shown in Figs. 6(a)–6(c), respectively. Both even and odd rotational states are periodically in phase for $\Phi = 0$ and $\Phi = \pi$ but only even rotational states line up in phase when $\Phi = 0.5\pi$ after the interaction. Therefore, there is no molecular orientation for the case of $\Phi = 0.5\pi$, as shown in

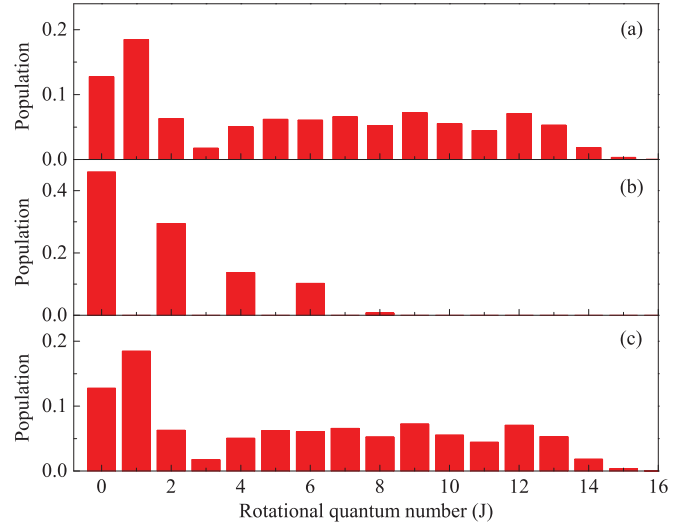


FIG. 6. (Color online) The populations of rotational states after the interaction with the femtosecond two-color laser pulse. (a) $\Phi = 0$, (b) 0.5π , and (c) $\Phi = \pi$.

Fig. 4. Thus, comparing with molecular alignment, the basic mechanism of molecular orientation is based on the creation of a rotational wave packet consisting of a superposition of even and odd rotational states in phase. If odd and even rotational states are out of phase by π , the orientation of both classes of states cancels out.

Furthermore, we calculate the time evolution of the phase for each rotational state. In Figs. 7(a) and 7(b) we show the phases φ of rotational states for $\Phi = 0$ and $\Phi = \pi$ at time E of Fig. 1, respectively. It is found that the phases for even rotation states are not changed but the phases for odd rotation states are shifted by $\Delta\varphi = \pi$, as shown in Fig. 7(c). This is the reason why the field-free molecular alignment for $\Phi = 0$ are the same as that of $\Phi = \pi$.

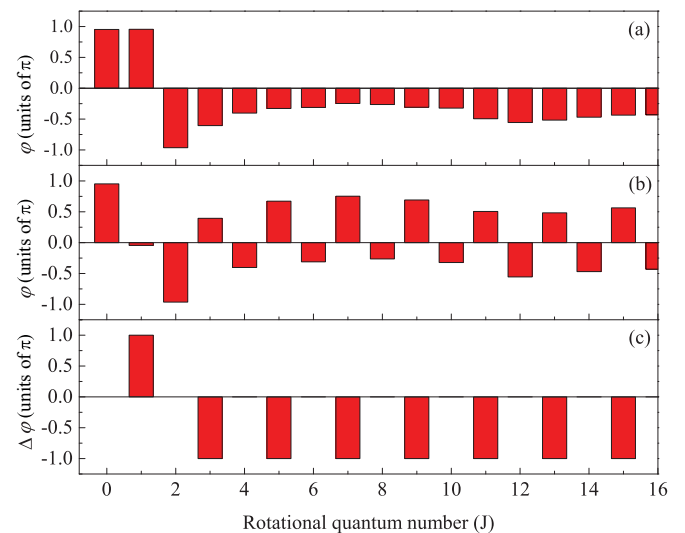


FIG. 7. (Color online) The phases φ of rotational states at time E in Fig. 1. (a) $\Phi = 0$, (b) π , and (c) the phase difference $\Delta\varphi$ of rotational states between $\Phi = 0$ and π .

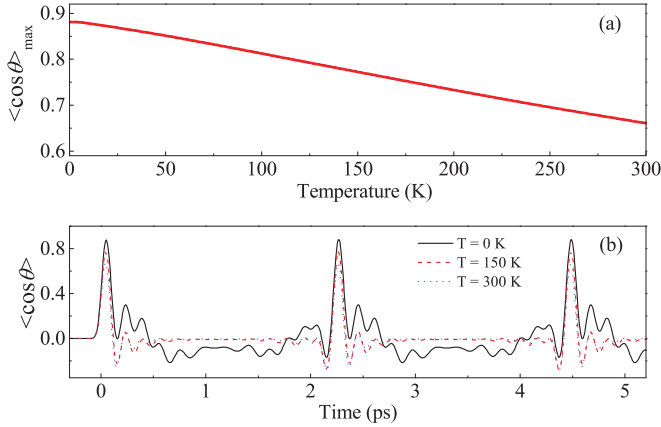


FIG. 8. (Color online) (a) Maximum degrees of molecular orientation and (b) time evolutions of thermally averaged orientation degree $\langle \cos \theta \rangle_T(t)$ at different initially rotational temperatures T .

The molecular alignment and orientation is influenced by the initial rotational temperature T . Since the molecules are considered initially as an incoherent ensemble, the ensemble average of the degree of molecular alignment and orientation over the initial angular momentum states is taken as

$$\langle \cos^n \theta \rangle_T(t) = \frac{\sum_J \exp[-BJ(J+1)/k_B T]}{\sum_J (2J+1) \exp[-BJ(J+1)/k_B T]} \times \sum_{M=-J}^J \langle \Psi_{JM}(t) | \cos^n \theta | \Psi_{JM}(t) \rangle, \quad (8)$$

where k_B is the Boltzmann constant, T is the initial rotational temperature, and Ψ_{JM} is the rotational wave function of the time-evolving molecule that has started the laser interaction in a state characterized by the angular quantum number J and the magnetic quantum number M . Figure 8(a) shows the maximum degree of molecular orientation $\langle \cos \theta \rangle_{\max}$ as a function of rotational temperature T , respectively. The molecular orientation reaches maximum nearby mT_{rot} ($m = 1, 2, 3, \dots$) for all the rotational temperatures T .

Since the revolution period of rotational states departs from T_{rot}/J due to centrifugal forces, the rate of angular dephasing will increase with the angular momentum J . Thus, the efficiency at higher temperatures is lower than at $T = 0$ K. However, we note that the maximal orientation does not change much from $\langle \cos \theta \rangle_{\max} = 0.881$ at $T = 0$ K to 0.661 at temperatures of $T = 300$ K, as shown in Fig. 8(b). Molecular alignment and molecular orientation depend similarly on temperature. In order to achieve the same degree of orientation as in the 0 K case, higher rotational states should be populated necessitating a more intense laser pulse.

We pointed out that we only choose one set of laser parameters, including wavelength, intensity, and duration. In principle, in order to achieve the maximum alignment or orientation, we could optimize all the above-mentioned

parameters. The two-color control has been widely adopted in the laboratory [28,29]. A subject for further investigation is to optimize the laser parameters or apply shaped laser fields or tailored excitation pulse sequences in order to increase the degree of orientation by two-color laser fields [40].

IV. CONCLUSION

We theoretically study the phase-dependent field-free molecular alignment and orientation of LiH by a femtosecond two-color laser pulse. The field-free molecular alignment and orientation exhibit a dependence on the phase between the components of femtosecond two-color laser pulse. A prospect is the control of the phase as a tool to steer the field-free molecular alignment and orientation. The explanation of the physical mechanism of the field-free molecular alignment and orientation induced by the femtosecond two-color laser pulse is that the populations of rotational states remain unchanged after the irradiation of laser field and the time evolution of phases play the most crucial role in determining the time evolution of molecular alignment and orientation. For the case of $\Phi = 0$ and $\Phi = \pi$ between the two components of the laser field molecular orientation and alignment are obtained, whereas for $\Phi = 0.5\pi$ only molecular alignment is established, in which only even rotational states are populated. The molecular alignment in the case of $\Phi = \pi$ is the same as that in the case of $\Phi = 0$ but orientation is different, which is due to the fact that in the case $\Phi = \pi$ the phases of even rotation states remain the same but the phases of odd rotation states shift by π , comparing with that of $\Phi = 0$. We also investigate the effect of rotational temperature on molecular alignment and orientation and propose a method for how an efficient field-free alignment and orientation can be realized even at room temperatures. Since the present technique depends on the nonresonant process, it can be applied to various molecules. The feasibility of the present approach has also been examined and the implementation of the present technique is now in progress in our laboratory.

ACKNOWLEDGMENTS

This work was supported by the National Natural Science Foundation of China (Grants No. 11304157, No. 11347116, No. U1404112, and No. 11404411), the Basic and Advanced Technology Research Program of Henan Province (Grants No. 12230041010, No. 142102310274, and No. 142300410168) and Swiss National Centre of Competence in Research, Molecular Ultrafast Science and Technology (NCCR-MUST). Y. Liu would also like to express thanks for the grants of International Fellowship Program (IFP-MUST) of the EU Marie Curie work program. We are also grateful to Dr. Patryk Jasik (Gdansk University of Technology, Gdansk) for offering the potential information of LiH and useful discussion.

[1] H. Stapelfeldt and T. Seideman, *Rev. Mod. Phys.* **75**, 543 (2003).
[2] T. Seideman, *Phys. Rev. Lett.* **83**, 4971 (1999).

[3] F. Rosca-Pruna and M. J. J. Vrakking, *Phys. Rev. Lett.* **87**, 153902 (2001).

- [4] Y. Tang, Y. I. Suzuki, T. Horio, and T. Suzuki, *Phys. Rev. Lett.* **104**, 073002 (2010).
- [5] J. J. Larsen, I. Wendt-Larsen, and H. Stapelfeldt, *Phys. Rev. Lett.* **83**, 1123 (1999).
- [6] C. Z. Bisgaard, O. J. Clarkin, G. R. Wu, A. M. D. Lee, O. Gessner, C. C. Hayden, and A. Stolow, *Science* **323**, 1464 (2009).
- [7] P. Hockett, C. Z. Bisgaard, O. J. Clarkin, and A. Stolow, *Nat. Phys.* **7**, 612 (2011).
- [8] J. Itatani, J. Levesque, D. Zeidler, H. Niikura, H. Pepin, J. C. Kieffer, P. B. Corkum, and D. M. Villeneuve, *Nature* **432**, 867 (2004).
- [9] H. Li, J. Liu, Y. H. Feng, C. Chen, H. F. Pan, J. Wu, and H. P. Zeng, *Appl. Phys. Lett.* **99**, 011108 (2011).
- [10] L. Holmegaard, J. L. Hansen, L. Kalhøj, S. L. Kragh, H. Stapelfeldt, F. Filsinger, J. Kupper, G. Meijer, D. Dimitrovski, M. Abu-samha, C. P. J. Martiny, and L. B. Madsen, *Nat. Phys.* **6**, 428 (2010).
- [11] D. H. Parker and R. B. Bernstein, *Annu. Rev. Phys. Chem.* **40**, 561 (1989).
- [12] B. Friedrich and D. R. Herschbach, *Nature* **353**, 412 (1991).
- [13] B. Friedrich and D. Herschbach, *J. Chem. Phys.* **111**, 6157 (1999).
- [14] C. Qin, Y. Tang, Y. Wang, and B. Zhang, *Phys. Rev. A* **85**, 053415 (2012).
- [15] C. C. Shu, K. J. Yuan, W. H. Hu, and S. L. Cong, *J. Chem. Phys.* **132**, 244311 (2010).
- [16] M. Machholm and N. E. Henriksen, *Phys. Rev. Lett.* **87**, 193001 (2001).
- [17] M. Lapert and D. Sugny, *Phys. Rev. A* **85**, 063418 (2012).
- [18] C. C. Shu and N. E. Henriksen, *Phys. Rev. A* **87**, 013408 (2013).
- [19] D. Daems, S. Guerin, D. Sugny, and H. R. Jauslin, *Phys. Rev. Lett.* **94**, 153003 (2005).
- [20] E. Gershnel, I. S. Averbukh, and R. J. Gordon, *Phys. Rev. A* **74**, 053414 (2006).
- [21] C. C. Shu, K. J. Yuan, W. H. Hu, J. Yang, and S. L. Cong, *Phys. Rev. A* **78**, 055401 (2008).
- [22] S. Fleischer, Y. Zhou, R. W. Field, and K. A. Nelson, *Phys. Rev. Lett.* **107**, 163603 (2011).
- [23] O. Ghafur, A. Rouzee, A. Gijsbertsen, W. K. Siu, S. Stolte, and M. J. J. Vrakking, *Nat. Phys.* **5**, 289 (2009).
- [24] H. Sakai, S. Minemoto, H. Nanjo, H. Tanji, and T. Suzuki, *Phys. Rev. Lett.* **90**, 083001 (2003).
- [25] L. Holmegaard, J. H. Nielsen, I. Nevo, H. Stapelfeldt, F. Filsinger, J. Kupper, and G. Meijer, *Phys. Rev. Lett.* **102**, 023001 (2009).
- [26] F. Filsinger, J. Kupper, G. Meijer, L. Holmegaard, J. H. Nielsen, I. Nevo, J. L. Hansen, and H. Stapelfeldt, *J. Chem. Phys.* **131**, 064309 (2009).
- [27] M. J. J. Vrakking and S. Stolte, *Chem. Phys. Lett.* **271**, 209 (1997).
- [28] S. De, I. Znakovskaya, D. Ray, F. Anis, N. G. Johnson, I. A. Bocharova, M. Magrakvelidze, B. D. Esry, C. L. Cocke, I. V. Litvinyuk, and M. F. Kling, *Phys. Rev. Lett.* **103**, 153002 (2009).
- [29] E. Frumker, C. T. Hebeisen, N. Kajumba, J. B. Bertrand, H. J. Worner, M. Spanner, D. M. Villeneuve, A. Naumov, and P. B. Corkum, *Phys. Rev. Lett.* **109**, 113901 (2012).
- [30] C. C. Qin, Y. Z. Liu, X. Z. Zhang, and Y. F. Liu, *Eur. Phys. J. D* **68**, 108 (2014).
- [31] T. Kanai and H. Sakai, *J. Chem. Phys.* **115**, 5492 (2001).
- [32] M. D. Feit, J. A. Fleck, and A. Steiger, *J. Comput. Phys.* **47**, 412 (1982).
- [33] Q. T. Meng, G. H. Yang, H. L. Sun, K. L. Han, and N. Q. Lou, *Phys. Rev. A* **67**, 063202 (2003).
- [34] T. S. Chu, Y. Zhang, and K. L. Han, *Int. Rev. Phys. Chem.* **25**, 201 (2006).
- [35] A. D. Bandrauk and H. Shen, *J. Chem. Phys.* **99**, 1185 (1993).
- [36] H. Yun, H. T. Kim, C. M. Kim, C. H. Nam, and J. Lee, *Phys. Rev. A* **84**, 065401 (2011).
- [37] H. Li, W. X. Li, Y. H. Feng, H. F. Pan, and H. P. Zeng, *Phys. Rev. A* **88**, 013424 (2013).
- [38] The potential energy curves of LiH are from the presentation of Dr. Patryk Jasik.
- [39] A. Sell, A. Leitenstorfer, and R. Huber, *Opt. Lett.* **33**, 2767 (2008).
- [40] S. A. Zhang, C. H. Lu, T. Q. Jia, Z. G. Wang, and Z. R. Sun, *Phys. Rev. A* **83**, 043410 (2011).